Available online at www.sciencedirect.com
ScienceDirect
Progress in Natural Science 18 (2008) 1271–1277
Progress in Natural Science
www.elsevier.com/locate/pnsc

Weighted LBF for spaceborne general bistatic SAR processing

Jinshan Ding [a,b,*], Otmar Loffeld [b], Robert Wang [b], Holger Nies [b], Ul-Ann Qurat [b], Zheng Bao [a]

[a] *The National Key Lab for Radar Signal Processing, Xidian University, Xi'an 710071, China*
[b] *The Center for Sensorsystems (ZESS), University of Siegen, Paul-Bonatz-Str. 9-11, Siegen 57076, Germany*

Received 17 January 2008; received in revised form 19 March 2008; accepted 25 March 2008

Abstract

Loffeld's bistatic formula (LBF) is the first two-dimensional analytic point target reference spectrum derived for general bistatic SAR frequency domain focusing. The phase history is expanded in Taylor series around the individual points of stationary phase of the transmitter-target and target-receiver phase histories, respectively, and thus the common bistatic stationary phase point can be obtained using the method of stationary phase. Unfortunately, it shows limitations for extreme bistatic configurations, namely the highly squinted mode and space-surface application. The weighted LBF (WLBF) is proposed in this paper based on the different contributions of total phase modulation from the transmitter and receiver. The formulae we derived are compared with that of the original literature. The extreme bistatic stripmap SAR data can be focused using WLBF, which accommodates the spaceborne squint geometry using the modified effective velocity solution. A point target simulation example is presented to verify the accuracy of the new WLBF spectrum.

Keywords: Bistatic SAR; SAR; Weighted LBF (WLBF); Hybrid bistatic configuration; Effective velocity approximation

1. Introduction

The physical separation of transmitter and receiver in bistatic systems has several advantages to the synthetic aperture radar (SAR) applications, such as the exploitation of extra information included in the bistatic reflectivity of targets and reduced vulnerability for military applications [1]. The bistatic SAR focusing is the first step for subsequent SAR applications, such as bistatic SAR interferometry for DEM and GMTI. Thus, effective focusing approaches are currently in the highlight of international SAR community.

Due to the intensive computational load of time domain back projection algorithms, SAR image formation processing is always preferred to be operated in the range Doppler or two-dimensional frequency domain for the exploitation of FFT efficiency. However, an exact analytic solution for the two-dimensional point target reference spectrum is difficult to find for bistatic SAR due to a double hyperbola in the bistatic range migration equation. Several solutions to the two-dimensional reference spectrum have been derived for bistatic SAR focusing, namely, Loffeld's bistatic formula (LBF) [2], an extended version of LBF that has been addressed partly in Ref. [3] for the hybrid configuration, the method of series reversion (MSR) and the geometry-based bistatic formulation (GBF) [4–6]. The MSR expands the bistatic range migration equation in a Taylor series, and by using the method of series reversion, the bistatic common stationary phase is derived successfully. The accuracy of stationary phase is determined by the number of incorporated terms in range migration equation expansion. The GBF succeeds in the exploitation of bistatic imaging geometry, and it avoids the Fourier integral with double hyperbola terms. The derived bistatic spectrum for general

* Corresponding author. Tel.: +49 271 740 2340; fax: +49 271 740 2336.
E-mail address: jinshanding@gmail.com (J. Ding).

1002-0071/$ - see front matter
doi:10.1016/j.pnsc.2008.03.022

bistatic SAR, LBF, contains a quasi-monostatic phase term and a bistatic deformation phase term. A few image formation algorithms have been developed based on LBF [7,8], which show excellent performance for moderate bistatic SAR data. Unfortunately, the performance of LBF-based algorithms is limited by the accuracy of the two-dimensional spectrum. Originally, LBF is obtained by applying a Taylor series expansion to the transmitter-target and target-receiver phase histories around the individual stationary phase up to the second order term. The inherent limitation lies in the compulsive averaging operation for the transmitter to target and target back to receiver phase histories. In this study, a weighted LBF (WLBF) is proposed. The accuracy of the WLBF spectrum for general spaceborne bistatic configuration is shown by the point target focusing simulation, where the effective velocity for spaceborne to airborne equivalent conversion is used for the accommodation of curved orbits [9,10].

2. Accommodation of spaceborne geometry

The general way to consider the orbital radar is to establish an earth-fixed reference system such that the origin is the Earth center. We use the well-known case in which the SAR platform follows a circular orbit around a spherical and non-rotating Earth [9,11]. The orbit eccentricity is small enough to consider the sensor velocity as a constant, at least in one synthetic aperture time [9,11,12]. A typical spaceborne bistatic SAR geometry is illustrated in Fig. 1. The transmitter and the receiver satellites are denoted as T and R, respectively; the transmitter to target and target back to receiver ranges at the zero azimuth time are denoted as R_{T0} and R_{R0}, respectively; H_T is the transmitter orbit height to the Earth center, and H_R the receiver; the Earth radius is R_e; and the space velocities are V_{ST} and V_{SR}. The orbits of transmitter and receiver satellite are not required to be parallel but can be arbitrary orbits in this study, although the footprints should overlap.

The spaceborne geometry concerning the effective velocity derivation is shown in Fig. 2, where only the transmitter satellite is present. Fig. 2(a) is on the normal plane to the orbit, i.e. plane APO in Fig. 2(b). The squint angle is denoted by ψ_{T0}.

The orbit orientation angle is α_T. The look angle of the radar beam center is denoted by γ_T, and the incident angle, an important design parameter for spaceborne SAR systems, is denoted by ϑ_T. The angle between the orbit plane and the Earth center to point target vector is φ_T. The effective velocity V_{ET} is given by

$$V_{ET} = \sqrt{V_{ST} V_{GT} \cos\psi_{T0}} = \sqrt{V_{ST}^2 \frac{R_e}{H_T} \sin(\alpha_T - \vartheta_T + \gamma_T) \cos\psi_{T0}} \quad (1)$$

where the squint spanned angle ψ_{T0} is always small even for highly squinted SAR. The effective velocity V_{ER} for receiver can be obtained in a similar way.

Note that the proposed modified effective velocity approximation is precise enough for spaceborne bistatic SAR simulations. For real data focusing at high resolution, a numerical calculation of the processing parameters can be used for high accuracy [10].

3. Bistatic signal model

By using the modified effective velocity approximation, the spaceborne bistatic geometry is well processed into an equivalent rectilinear path geometry model. A slightly modified point of closest approach (PCA) should be used for high accuracy [9]. In what follows, we use the equivalent airborne geometry to model the signal of bistatic SAR.

The equivalent airborne geometry is shown in Fig. 3 for derivation.

The transmitter and receiver squint angles with respect to target are denoted by θ_{T0} and θ_{R0}, respectively, assumed at zero azimuth time as shown in Fig. 3. The PCAs are R_{BT}

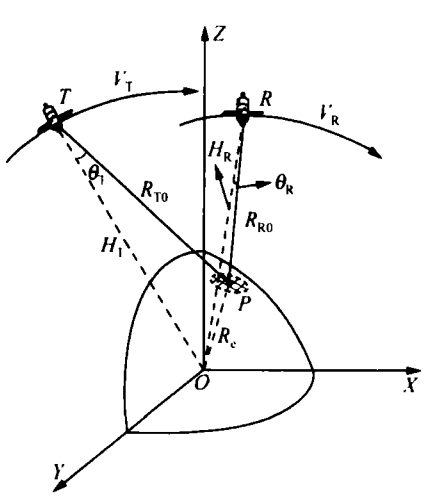

Fig. 1. Spaceborne general bistatic SAR geometry for signal modeling.

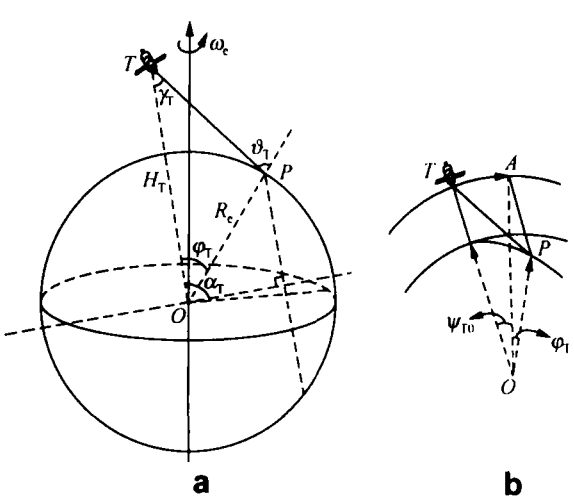

Fig. 2. Spaceborne geometry for modified effective velocity derivation.

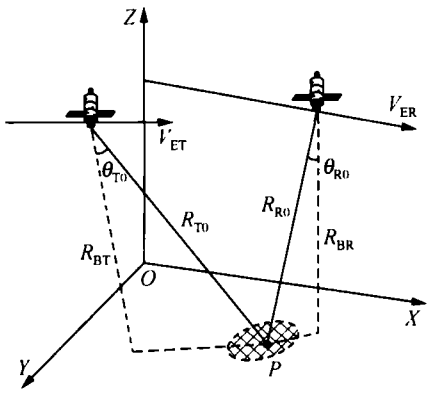

Fig. 3. Equivalent airborne bistatic SAR geometry illustration.

and R_{BR}, respectively. Thus, the bistatic slant range, $R(\eta)$, can be written as

$$R(\eta) = R_T(\eta) + R_R(\eta) \tag{2}$$

where $R_T(\eta) = \sqrt{R_{BT}^2 + (V_{ET}\eta - V_{ET}\eta_{T0})^2}$ and $R_R(\eta) = \sqrt{R_{BR}^2 + (V_{ER}\eta - V_{ER}\eta_{R0})^2}$. The azimuth slow time offsets are denoted by $\eta_{T0} = R_{BT}\tan\theta_{T0}/V_{ET}$ and $\eta_{R0} = R_{BR}\tan\theta_{R0}/V_{ER}$.

Suppose a chirp transmitted waveform, after downconversion to baseband, the echo signal is

$$s(t,\eta) = p\left(t - \frac{R(\eta)}{c}\right) w_{az}(\eta) \times \exp\left(j\pi\gamma\left(t - \frac{R(\eta)}{c}\right)^2\right) \exp\left(-j2\pi\frac{R(\eta)}{\lambda}\right) \tag{3}$$

where t is the range fast time, $p(t)$ is the pulse envelope, γ is the range frequency rate, λ is the radar center wavelength, and $w_{az}(\eta)$ is the azimuth pattern function. After range compression and range Fourier transformation, the range frequency domain signal is

$$s(f_r,\eta) = W_r(f_r) w_{az}(\eta) \exp\left(-j2\pi(f_c + f_r)\frac{R(\eta)}{c}\right) \tag{4}$$

where $W_r(f_r)$ is the range spectrum shape, and f_c and f_r are radar center frequency and range frequency, respectively. To obtain the two-dimensional spectrum, we take the azimuth Fourier transformation to (4)

$$s(f_r,f_\eta) = W_r(f_r)\int w_{az}(\eta) \times \exp\left(-j2\pi(f_c + f_r)\frac{R(\eta)}{c}\right) \exp(-j2\pi f_\eta\eta)\,d\eta \tag{5}$$

where f_η is azimuth Doppler frequency.

The link between the slow time and Doppler frequency is

$$f_\eta = -\frac{f_c + f_r}{c}\dot{R}(\eta) \tag{6}$$

To obtain the analytic point target spectrum, the Fourier integral in (5) should be resolved, which is the goal of all proposed methods, such as LBF and MSR.

4. Weighted LBF

The original LBF divides the bistatic phase in (5) into two parts contributed by the transmitter and receiver, respectively. The two parts are counted in the Fourier integral of (5) identically. The two phases are written as [2]

$$\phi_T(\eta) = 2\pi(f_c + f_r)R_T(\eta)/c + \pi f_\eta\eta \tag{7a}$$

$$\phi_R(\eta) = 2\pi(f_c + f_r)R_R(\eta)/c + \pi f_\eta\eta \tag{7b}$$

The limitation of original LBF is due to the compulsive averaging operation for the transmitter to target and target back to receiver phase histories, which motivates the modification of LBF. The bistatic phase history is expanded around the individual transmitting and receiving stationary phase points, respectively, by using an adaptive weight instead of the average. The weight is determined by the different contributions in bistatic phase history from the transmitter and receiver, that is, the Doppler frequency rate in azimuth. This method is straightforward in principle, that is, the common bistatic stationary phase should be determined by different contributions of transmitter and receiver.The normalized weight W can be written in vector

$$W = \begin{bmatrix} W_T \\ W_R \end{bmatrix} = \begin{bmatrix} \frac{|\gamma_T|}{|\gamma_T|+|\gamma_R|} \\ \frac{|\gamma_R|}{|\gamma_T|+|\gamma_R|} \end{bmatrix} \tag{8}$$

where γ_T and γ_R are Doppler frequency modulation rates evaluated at the beam center time from the transmitter and receiver, respectively. We have the Doppler rates as

$$\gamma_T = \frac{-V_{ET}^2\cos^2\theta_{T0}}{\lambda R_{T0}}, \quad \gamma_R = \frac{-V_{ER}^2\cos^2\theta_{R0}}{\lambda R_{R0}} \tag{9}$$

Thus, the weighted two phase terms can be rewritten as

$$\phi_T(\eta) = 2\pi(f_c + f_r)R_T(\eta)/c + W_T 2\pi f_\eta\eta \tag{10a}$$

$$\phi_R(\eta) = 2\pi(f_c + f_r)R_R(\eta)/c + W_R 2\pi f_\eta\eta \tag{10b}$$

The above phases are expanded into two Taylor series around the individual stationary phase points. By keeping up to the second-order term, we have

$$\phi_T = \phi_T(\tilde{\eta}_T) + \dot{\phi}_T(\tilde{\eta}_T)(\eta - \tilde{\eta}_T) + \frac{1}{2}\ddot{\phi}_T(\tilde{\eta}_T)(\eta - \tilde{\eta}_T)^2 \tag{11a}$$

$$\phi_R = \phi_R(\tilde{\eta}_R) + \dot{\phi}_R(\tilde{\eta}_R)(\eta - \tilde{\eta}_R) + \frac{1}{2}\ddot{\phi}_R(\tilde{\eta}_R)(\eta - \tilde{\eta}_R)^2 \tag{11b}$$

According to the definition of stationary phase, the first-order terms vanish in (11). We have the bistatic phase ϕ_b as

$$\phi_b = \phi_R(\tilde{\eta}_R) + \frac{1}{2}\ddot{\phi}_R(\tilde{\eta}_R)(\eta - \tilde{\eta}_R)^2 + \phi_T(\tilde{\eta}_T) + \frac{1}{2}\ddot{\phi}_T(\tilde{\eta}_T)(\eta - \tilde{\eta}_T)^2 \tag{12}$$

where $\phi_R(\tilde{\eta}_R)$ and $\phi_T(\tilde{\eta}_T)$ are constants and can be carried out of the integral sign. The remaining Fourier integral phase in (5) is

$$I = \int w_{az}(\eta) \times \exp\left\{-j\frac{1}{2}\left[\ddot{\phi}_R(\tilde{\eta}_R)(\eta-\tilde{\eta}_R)^2 + \ddot{\phi}_T(\tilde{\eta}_T)(\eta-\tilde{\eta}_T)^2\right]\right\} d\eta \tag{13}$$

By using the method of stationary phase, we obtain the bistatic common stationary phase point $\tilde{\eta}$ as

$$\tilde{\eta} = \frac{\ddot{\phi}_T(\tilde{\eta}_T)\tilde{\eta}_T + \ddot{\phi}_R(\tilde{\eta}_R)\tilde{\eta}_R}{\ddot{\phi}_T(\tilde{\eta}_T) + \ddot{\phi}_R(\tilde{\eta}_R)} \tag{14}$$

Consequently, we obtain the result of (13) as

$$I = W_{az}(f_\eta)\frac{\sqrt{2\pi}\cdot e^{-j\frac{\pi}{4}}}{\sqrt{\ddot{\phi}_T(\tilde{\eta}_T) + \ddot{\phi}_R(\tilde{\eta}_R)}} \times \exp\left\{-j\frac{1}{2}\frac{\ddot{\phi}_T(\tilde{\eta}_T)\ddot{\phi}_R(\tilde{\eta}_R)}{\ddot{\phi}_T(\tilde{\eta}_T) + \ddot{\phi}_R(\tilde{\eta}_R)}(\tilde{\eta}_T - \tilde{\eta}_R)^2\right\} \tag{15}$$

We have the final point target spectrum (WLBF)

$$s(f_\tau, f_\eta) = W_r(f_\tau)W_{az}(f_\eta)\frac{\sqrt{2\pi}}{\sqrt{\ddot{\phi}_T(\tilde{\eta}_T) + \ddot{\phi}_R(\tilde{\eta}_R)}}e^{-j\frac{\pi}{4}} \cdot \exp\{-j[\phi_R(\tilde{\eta}_R) + \phi_T(\tilde{\eta}_T)]\} \cdot \exp\left\{-j\frac{1}{2}\frac{\ddot{\phi}_T(\tilde{\eta}_T)\ddot{\phi}_R(\tilde{\eta}_R)}{\ddot{\phi}_T(\tilde{\eta}_T) + \ddot{\phi}_R(\tilde{\eta}_R)}(\tilde{\eta}_T - \tilde{\eta}_R)^2\right\} \tag{16}$$

where $W_{az}(f_\eta)$ is the shape of azimuth spectrum. The amplitude factors can be neglected for the only image formation purpose.

4.1. Receiver parameter derivation

We have to calculate the parameters related to receiver and transmitter that are used in the WLBF. From (10b), we have the first and the second order derivatives of receiver phase as

$$\dot{\phi}_R(\eta) = 2\pi(f_c + f_\tau)\dot{R}_R(\eta)/c + W_R 2\pi f_\eta \tag{17}$$

$$\ddot{\phi}_R(\eta) = 2\pi(f_c + f_\tau)\ddot{R}_R(\eta)/c \tag{18}$$

Thus, the derivative of receiver slant range should be calculated. After some mathematics, we have the following results

$$\dot{R}_R(\eta) = V_{ER}^2\frac{\eta - \eta_{R0}}{R_R(\eta)} \tag{19}$$

$$\ddot{R}_R(\eta) = \frac{V_{ER}^2}{R_R(\eta)} - \frac{V_{ER}^4}{R_R^3(\eta)}(\eta - \eta_{R0})^2 \tag{20}$$

Using the principle of stationary phase in (17) yields

$$\dot{\phi}_R(\tilde{\eta}_R) = 2\pi(f_c + f_\tau)\dot{R}_R(\tilde{\eta}_R)/c + W_R 2\pi f_\eta = 0 \tag{21}$$

Substituting (19) into (21), we obtain

$$\tilde{\eta}_R - \eta_{R0} = -W_R \cdot f_\eta R_R(\tilde{\eta}_R)\frac{c}{V_{ER}^2(f_c + f_\tau)} \tag{22}$$

From $R_R(\eta) = \sqrt{R_{BR}^2 + (V_{ER}\eta - V_{ER}\eta_{R0})^2}$, we have $V_{ER}^2(\tilde{\eta}_R - \eta_{R0})^2 = R_R^2(\tilde{\eta}_R) - R_{BR}^2$. Thus, we obtain

$$R_R(\tilde{\eta}_R) = R_{BR}\frac{|f_c + f_\tau|}{\sqrt{(f_c + f_\tau)^2 - \frac{W_R^2 f_\eta^2 c^2}{V_{ER}^2}}} \tag{23}$$

We define two notations for simplicity in derivation

$$F_R(f_\tau, f_\eta) = (f_\tau + f_c)^2 - \frac{W_R^2 f_\eta^2 c^2}{V_{ER}^2}$$
$$F_T(f_\tau, f_\eta) = (f_\tau + f_c)^2 - \frac{W_T^2 f_\eta^2 c^2}{V_{ET}^2} \tag{24}$$

Eq. (23) can be rewritten as

$$R_R(\tilde{\eta}_R) = R_{BR}\frac{|f_c + f_\tau|}{F_R^{\frac{1}{2}}(f_\tau, f_\eta)} \tag{25}$$

And the receiver stationary phase point can be expressed as

$$\tilde{\eta}_R = \eta_{R0} - \frac{W_R f_\eta c}{V_{ER}^2}\cdot R_{BR}\frac{\mathrm{sgn}(f_c + f_\tau)}{F_R^{\frac{1}{2}}(f_\tau, f_\eta)} \tag{26}$$

where the sign function is defined as

$$\mathrm{sgn}(x) = \begin{cases} 1, & x > 0 \\ 0, & x = 0 \\ -1, & x < 0 \end{cases}$$

As the next step, the value of the second-order derivative of the receiver phase at the stationary phase point should be calculated. According to (19) and (20), we have

$$\ddot{R}_R(\tilde{\eta}_R) = \frac{V_{ER}^2 - \dot{R}_R(\tilde{\eta}_R)^2}{R_R(\tilde{\eta}_R)} \tag{27}$$

From (19) and (22), we also have the relationship at the receiver's stationary phase point

$$\dot{R}_R(\tilde{\eta}_R) = \frac{V_{ER}^2(\tilde{\eta}_R - \eta_{R0})}{R_R(\tilde{\eta}_R)} = -\frac{W_R f_\eta c}{f_c + f_0} \tag{28}$$

Inserting the above expression into (27), we obtain

$$\ddot{R}_R(\tilde{\eta}_R) = \frac{V_{ER}^2 - \left[\frac{W_R f_\eta c}{(f_c + f_\tau)}\right]^2}{R_{BR}|f_c + f_\tau|}\sqrt{(f_c + f_\tau)^2 - \frac{W_R^2 f_\eta^2 c^2}{V_{ER}^2}} = \frac{V_{ER}^2}{R_{BR}}\frac{\left[(f_c + f_\tau)^2 - \frac{W_R^2 f_\eta^2 c^2}{V_{ER}^2}\right]^{\frac{3}{2}}}{|f_c + f_\tau|(f_c + f_\tau)^2} \tag{29}$$

From (18), we get the second-order derivative of receiver phase at the stationary phase point

$$\ddot{\phi}_R(\tilde{\eta}_R) = \frac{2\pi}{c}\frac{V_{ER}^2}{R_{BR}}\frac{F_R^{\frac{3}{2}}\mathrm{sgn}(f_c+f_r)}{(f_c+f_r)^2} \tag{30}$$

In addition, the receiver's phase term at the receiver's point of stationary phase is given by

$$\phi_R(\tilde{\eta}_R) = 2\pi W_R f_\eta \eta_{R0} + \frac{2\pi}{c}\mathrm{sgn}(f_c+f_r)R_{BR}F_R^{\frac{1}{2}} \tag{31}$$

4.2. Transmitter parameter derivation

The derivation of transmitter related parameters is similar to that mentioned above. However, we introduce two notations for transmitter parameters calculation as that in Ref. [2], which describe the bistatic grade of bistatic SAR system. The first is the slow time offset of transmitter and receiver at the point of closest approaches, i.e. a_0

$$a_0 = \eta_{T0} - \eta_{R0} \tag{32}$$

and the second is the ratio of transmitter and receiver closest approaches, a_2

$$a_2 = \frac{R_{BT}}{R_{BR}} \tag{33}$$

The needed parameters can be derived as follows

$$R_T(\tilde{\eta}_T) = R_{BR}a_2\frac{|f_c+f_r|}{F_T^{\frac{1}{2}}(f_r,f_\eta)} \tag{34}$$

$$\tilde{\eta}_T - \eta_{R0} = -\frac{W_T f_\eta c}{V_{ET}^2}\frac{R_{BR}\mathrm{sgn}(f_c+f_r)a_2}{\sqrt{(f_c+f_r)^2 - \frac{W_T^2 f_\eta^2 c^2}{V_{ET}^2}}} + a_0 \tag{35}$$

Thus, we have the final point of stationary phase of transmitter

$$\tilde{\eta}_T = \eta_{R0} + a_0 - \frac{W_T f_\eta c}{V_{ET}^2}\cdot R_{BR}a_2\frac{\mathrm{sgn}(f_c+f_r)}{F_T^{\frac{1}{2}}(f_r,f_\eta)} \tag{36}$$

Similarly, we have the transmitter's phase

Table 1
Simulation parameters

Parameter	Transmitter	Receiver 1	Receiver 2
Space velocity	7604.9 m/s	7451.9 m/s	120 m/s
Orbit height	514 km	800 km	5 km
Center frequency	10 GHz	10 GHz	10 GHz
Bandwidth	50 MHz	50 MHz	50 MHz
Pulse duration	5 μs	5 μs	5 μs
Angle between velocity vectors	4°		5°
Transmitter closest approach	800 km		
Receiver closest approach		1200 km	8 km
Baseline at receiver's PCA		400 km	600 km
Antenna aperture	8 m	10 m	0.5 m

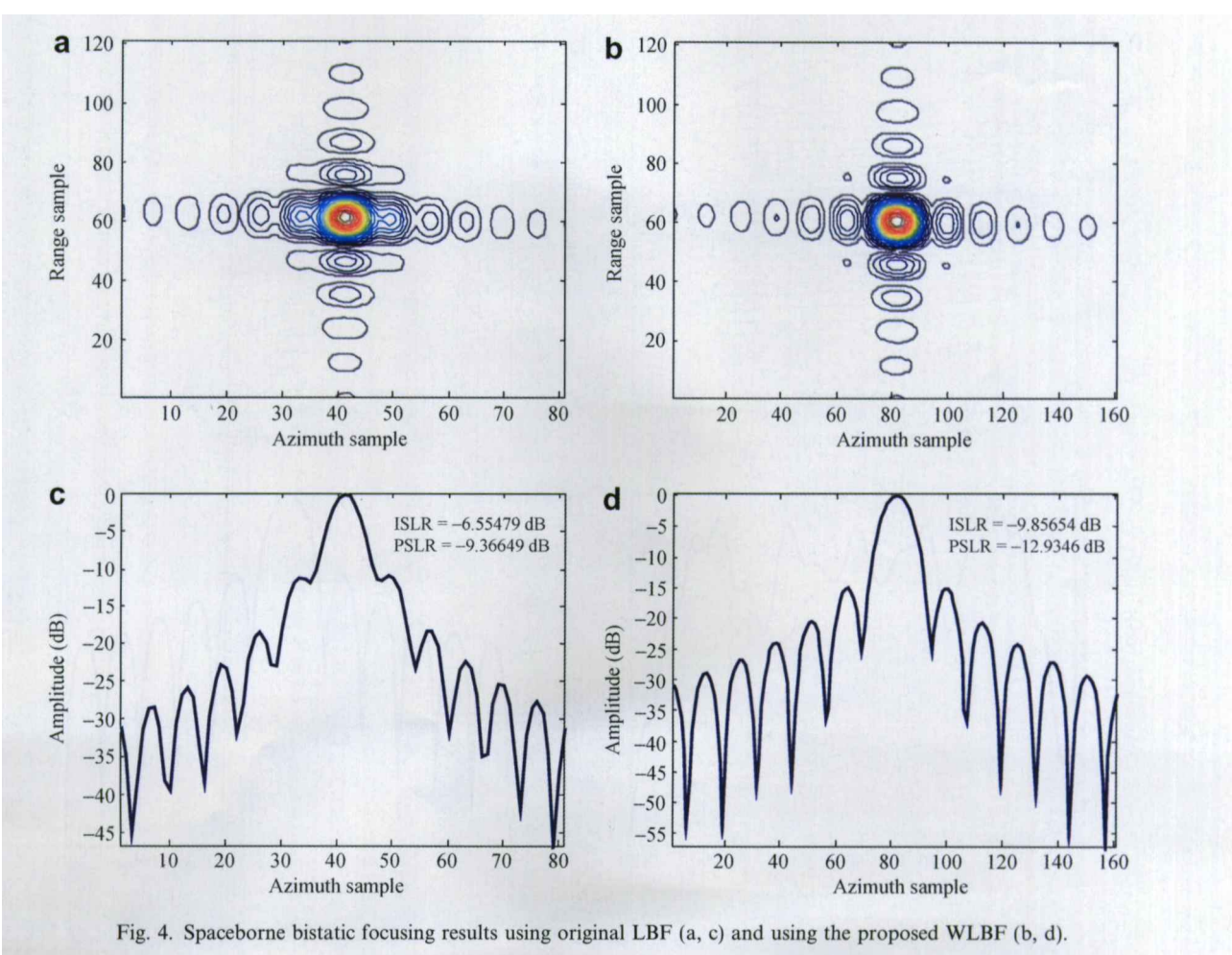

Fig. 4. Spaceborne bistatic focusing results using original LBF (a, c) and using the proposed WLBF (b, d).

$$\phi_T(\tilde{\eta}_T) = 2\pi W_T f_\eta(\eta_{R0} + a_0) + \frac{2\pi}{c}\mathrm{sgn}(f_c + f_r)F_T^{\frac{1}{2}}R_{BR}a_2 \tag{37}$$

and the transmitter second-order derivative at the point of stationary phase is

$$\ddot{\phi}_T(\tilde{\eta}_T) = 2\pi\frac{\mathrm{sgn}(f_c + f_r)}{cR_{BR}a_2}\cdot\frac{V_{ET}^2F_T(f_r,f_\eta)^{\frac{3}{2}}}{(f_c + f_r)^2} \tag{38}$$

The slow time difference of transmitter and receiver points of stationary phases is given by

$$\tilde{\eta}_T - \tilde{\eta}_R = a_0 - \frac{f_\eta c\cdot\mathrm{sgn}(f_c + f_r)R_{BR}}{V_{ET}^2V_{ER}^2}\cdot\left[\frac{W_TV_{ER}^2F_R^{\frac{1}{2}}(f_r,f_\eta)a_2 - W_RV_{ET}^2F_T^{\frac{1}{2}}(f_r,f_\eta)}{F_T^2(f_r,f_\eta)F_R^2(f_r,f_\eta)}\right] \tag{39}$$

4.3. WLBF

The quasi-monostatic phase term of WLBF is given by

$$\psi_m = \phi_T(\tilde{\eta}_T) + \phi_R(\tilde{\eta}_R) = 2\pi f_\eta[W_R\eta_{R0} + W_T(\eta_{R0} + a_0)] + \frac{2\pi R_{BR}\mathrm{sgn}(f_c + f_r)}{c}\left[F_R^{\frac{1}{2}} + F_T^{\frac{1}{2}}a_2\right] \tag{40}$$

The bistatic deformation term is

$$\psi_b = \frac{1}{2}\frac{\ddot{\phi}_T(\tilde{\eta}_T)\ddot{\phi}_R(\tilde{\eta}_R)}{\ddot{\phi}_T(\tilde{\eta}_T) + \ddot{\phi}_R(\tilde{\eta}_R)}(\tilde{\eta}_T - \tilde{\eta}_R)^2 = \frac{\pi\mathrm{sgn}(f_c + f_r)}{R_{BR}(f_c + f_r)^2c}V_{ET}^2V_{ER}^2\cdot\frac{F_R^{\frac{3}{2}}F_T^{\frac{3}{2}}}{F_R^{\frac{3}{2}}V_{ER}^2a_2 + V_{ET}^2F_T^{\frac{3}{2}}}\cdot\left\{a_0 - \frac{f_\eta c\cdot\mathrm{sgn}(f_c + f_r)R_{BR}}{V_{ET}^2V_{ER}^2}\left[\frac{W_TV_{ER}^2F_R^{\frac{1}{2}}a_2 - W_RV_{ET}^2F_T^{\frac{1}{2}}}{F_T^{\frac{1}{2}}F_R^{\frac{1}{2}}}\right]\right\}^2 \tag{41}$$

Finally, we rewrite the weighted LBF for general bistatic SAR as

$$s(f_r,f_\eta) = W_r(f_r)W_{az}(f_\eta)\frac{\sqrt{2\pi}}{\sqrt{\ddot{\phi}_T(\tilde{\eta}_T) + \ddot{\phi}_R(\tilde{\eta}_R)}}e^{-j\frac{\pi}{4}}\cdot\exp\{-j\psi_m\}\exp\{-j\psi_b\} \tag{42}$$

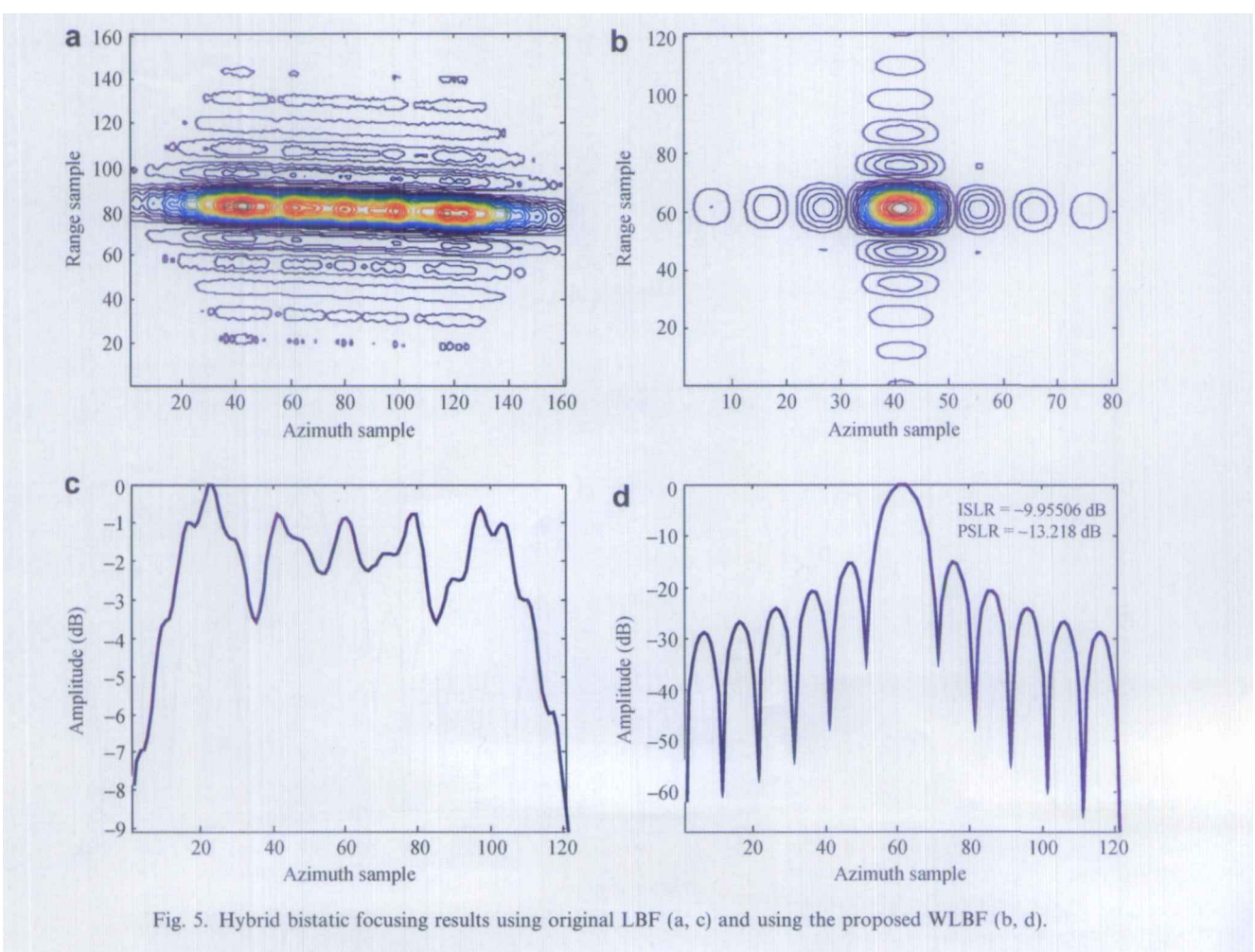

Fig. 5. Hybrid bistatic focusing results using original LBF (a, c) and using the proposed WLBF (b, d).

5. Accuracy of WLBF

To verify the accuracy of the new proposed point target spectrum for general spaceborne bistatic SAR, two point target focusing examples are presented. The first is a spaceborne bistatic SAR system works in a high squint mode where the receiver is supposed to be in the side looking mode and the transmitter follows the footprint of transmitter. The second simulation is based on a spaceborne hybrid bistatic SAR constellation proposed in Ref. [13], an extreme bistatic SAR configuration where the TerraSAR-X radar serves as the transmitter and an airborne platform PAMIR is used as the receiver. The simulation parameters are given in Table 1. The effective velocities of transmitter and receiver are calculated according to (1). The bistatic squint angle for case 1 is 15°.

The focusing results are illustrated in Fig. 4 for spaceborne and in Fig. 5 for hybrid configuration by using the original LBF and the proposed weighted LBF, respectively. No window is used in the processing.

From Fig. 4, we can see that the focusing of point-like target is improved. Due to the second-order Taylor expansion used in (11), the WLBF shares the same limitation to achieve the ideal focusing as the original LBF.

As for the spaceborne airborne hybrid bistatic configuration, the bistatic squint angle is as small as 1.7°. The original LBF shows great limitation due to the significant difference in velocities, i.e. 7905.1 m/s and 120 m/s.

From Fig. 5, we can see that the focusing is dramatically improved. The original LBF defocuses completely. The weighted LBF can deal with this extreme bistatic SAR configuration sufficiently.

6. Conclusion

The WLBF can be used to process the spaceborne SAR data as well as the airborne data with or without the proposed effective velocity approximation. Based on the WLBF point target spectrum, the derived algorithms using conventional LBF [7,8] can be well used to focus general bistatic SAR data, which will not be repeated here. The proposed weighted LBF approach can be also used to process the data from the squint spaceborne bistatic case and the spaceborne airborne hybrid bistatic case, where the transmitter-target and target back to receiver phase histories show an extreme difference.

The modified effective velocity approximation has been presented in this paper to accommodate the bistatic spaceborne geometry. This method is sufficient for most cases of radar parameters, such as the used center frequency and required azimuth resolution. For large orbital arc due to small antenna and long wavelength, the solution to spaceborne bistatic SAR signal modeling needs further study.

Acknowledgments

This work was supported by the National Natural Science Foundation of China (Grant No. 60502044) and the program of NCET (Grant No. NCET-06-0861). The authors would like to thank the Chinese Scholarship Council for providing scholarship funding for Jinshan Ding. Thanks also go to Dr. Stefan Knedlik for his support in ZESS and to Professor Mengdao Xing for his support in the research of bistatic SAR.

References

[1] Krieger G, Moreira A. Spaceborne bi- and multistatic SAR: potential and challenges. IEE Proc-Radar Sonar Navig 2006;153(6):184–98.
[2] Loffeld O, Nies H, Peters V, et al. Models and useful relations for bistatic SAR. IEEE Trans Geosci Remote Sensing 2004;42(10):2031–8.
[3] Wang R, Loffeld O, Qurat U, et al. Analysis and extension of Loffeld's bistatic formula for the spaceborne/airborne configuration. In: The Proceedings of European SAR Conference, Friedrichshafen, Germany, June, 2008.
[4] Wang R, Loffeld O, Nies H, et al. A special point target reference spectrum for spaceborne/airborne configuration. In: The Proceedings of European SAR Conference, Friedrichshafen, Germany, June, 2008.
[5] Neo Y, Wong F, Cumming I. A two-dimensional spectrum for bistatic SAR processing using series reversion. IEEE Geosci Remote Sensing Lett 2007;4(1):93–6.
[6] Zhang ZH, Xing MD, Ding JS, et al. Focusing parallel bistatic SAR data using the analytic transfer function in wavenumber domain. IEEE Trans Geosci Remote Sensing 2007;45(11):3633–45.
[7] Natroshvili K, Loffeld O, Amaya O, et al. Focusing of general bistatic SAR configuration data with 2-D inverse scaled FFT. IEEE Trans Geosci Remote Sensing 2006;44(10):2718–27.
[8] Nies H, Loffeld O, Natroshvili K. Analysis and focusing of bistatic airborne SAR data. IEEE Trans Geosci Remote Sensing 2007;45(11):3324–49.
[9] Cumming I, Wong F. Digital processing of synthetic aperture radar data: algorithms and implementation. MA: Artech House; 2005.
[10] Wong F, Tan N, Yeo T. Effective velocity estimation for spaceborne SAR. In: Proceedings of IEEE Geoscience and Remote Sensing Symposium, Singapore, 2000, pp. 90–2.
[11] Raney R. Doppler properties of radars in circular orbits. Int J Remot Sens 1986;7(9):1153–62.
[12] Davidson G, Cumming I. Signal properties of spaceborne squint-mode SAR. IEEE Trans Geosci Remote Sensing 1997;35(3):611–7.
[13] Walterscheid I, Klare J, Brenner A, et al. Challenges of a bistatic spaceborne/airborne SAR experiment. In: Proceedings of European SAR Conference, Dresden, Germany, May, 2006.